Research on the mechanism of the threefold discrepancy in thermal conductivity between room temperature and phase transition temperature for 1,3,5,7-tetranitro-1,3,5,7-tetrazocine (HMX) crystals

He Wang[a#], Wentao Liang[a#], Xiangqi Wang[b], Hao Wang[a], Di Mai[a], Cheng Zhong[a], Xiaoyu Sun[c], Rucheng Dai[c], Zhongping Wang[c], Xianxu Zheng[d*], Wanguo Zheng[e*] and Zengming Zhang[c*]

[a] Department of Physics, School of Physics Science, University of Science and Technology of China, Hefei, Anhui, 230026, China

[b] Ji Hua Laboratory Testing Center, Ji Hua Laboratory, Foshan, Guangdong 528000, China

[c] The Center for Physical Experiments, School of Physics Science, University of Science and Technology of China, Hefei, Anhui, 230026, China

[d] Institute of Fluid Physics, China Academy of Engineering Physics, Mianyang, Sichuan 621900, China

[e] Research Center of Laser Fusion, China Academy of Engineering Physics, Mianyang Sichuan 621900, China

[*] Email: zxxgoal109@sina.com, for X. Z.

[*] Email: yehanwin@mail.ustc.edu.cn, for W. Z.

[*] Email: zzm@ustc.edu.cn, for Z. Z.

[#] H. W. and W. L. contributed equally to this paper

List of Contents

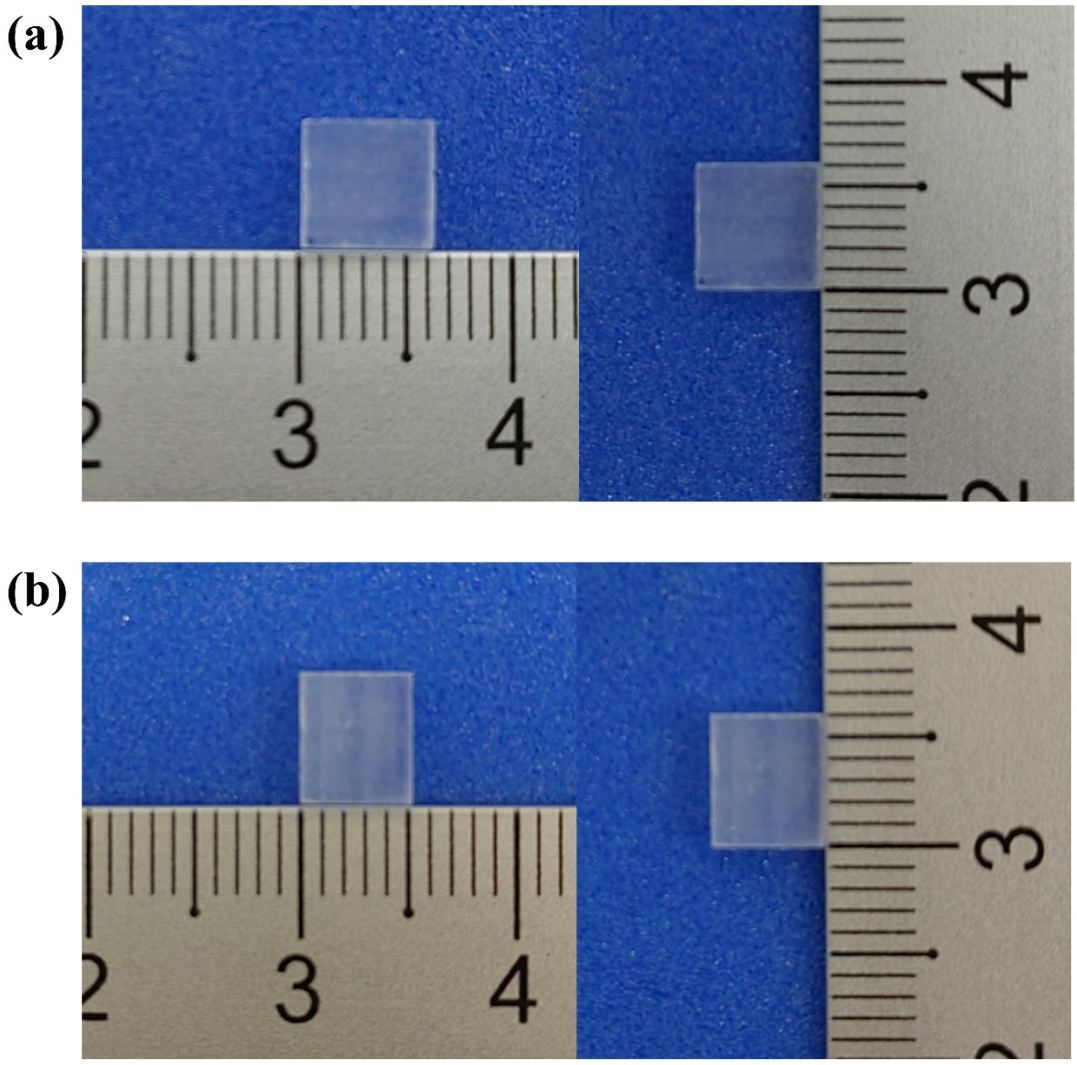

Figure S1 Two sizes of the HMX single crystals. (a) Type a with a size of 6 mm × 6 mm × 1.5 mm. (b) type b with dimensions of 5 mm × 6 mm × 1.5 mm

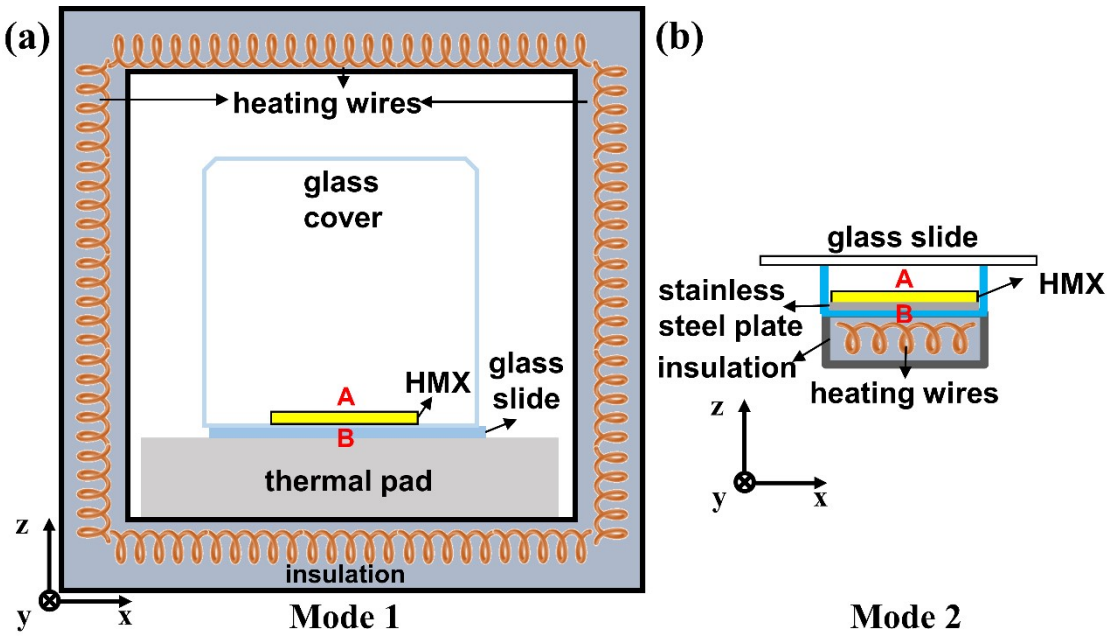

Figure S2 Two modes of heating. (a) Evenly heated by a BEQ MF-1100C furnace. (b) The sample was heated by a Linkam TS1500 high-temperature heat stage with a glass slide on top, allowing for a temperature gradient from the bottom to the top of the sample.

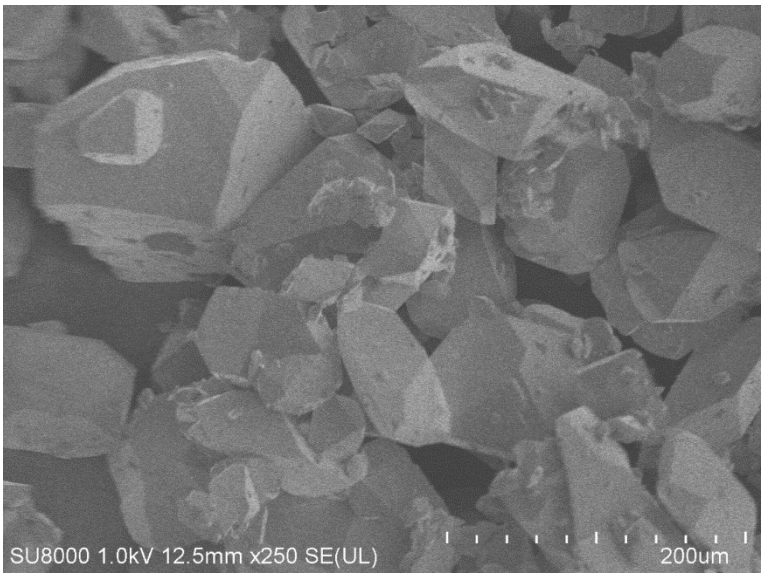

Figure S3 The scanning electron microscope (SEM) image of β-HMX powder

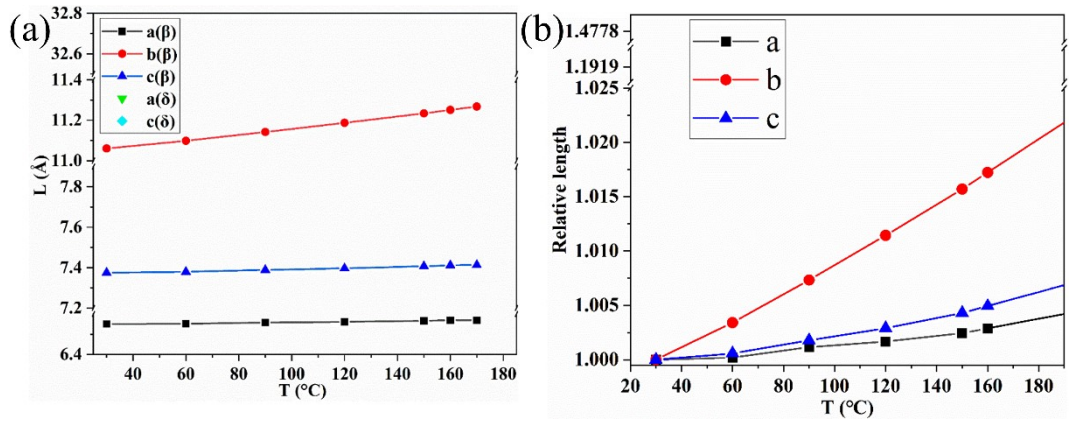

Figure S4 (a)Variation of lattice parameter of β-HMX with temperature (b) Relative change of lattice parameters of β-HMX with temperature, all lattice parameters are normalized to those at 30 °C.

.

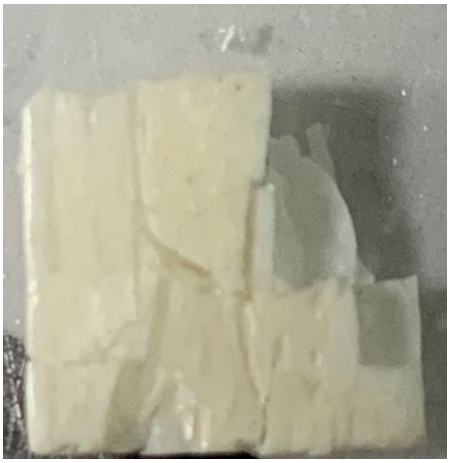

Figure S5 Image of P2 broken after being heated. The holding time at 185°C was 15 min, and the other heating conditions were consistent with those used for P3.

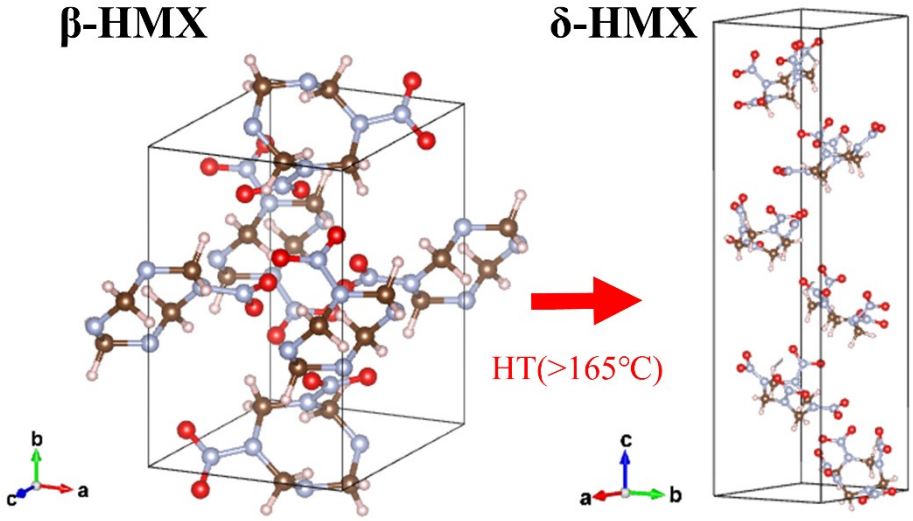

Figure S6 Schematic diagram of phase transition from β-HMX to δ-HMX, HT stands for high temperature.

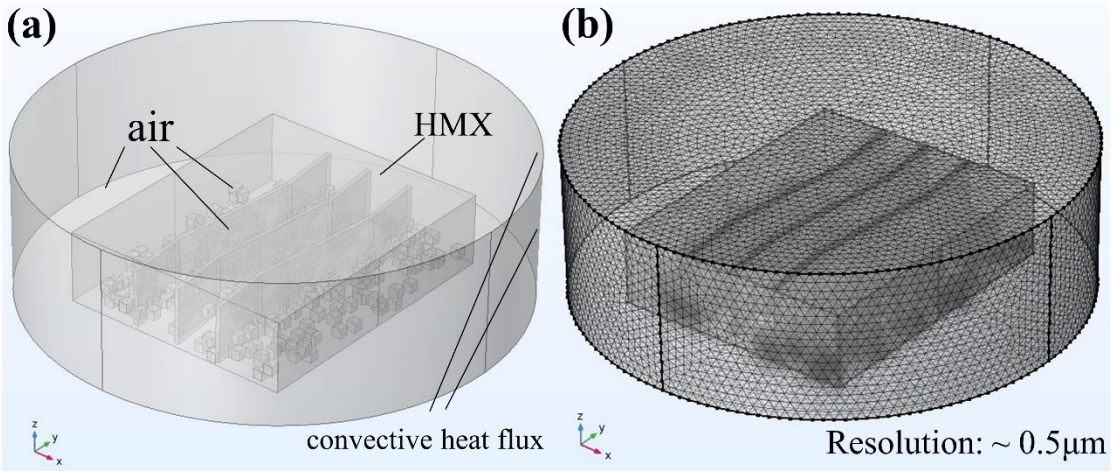

Figure S7 (a) Illustration of HMX crystal in high temperature furnace mode. (b) Finite element meshing of the model with a minimum unit size of about 0.5 μm.

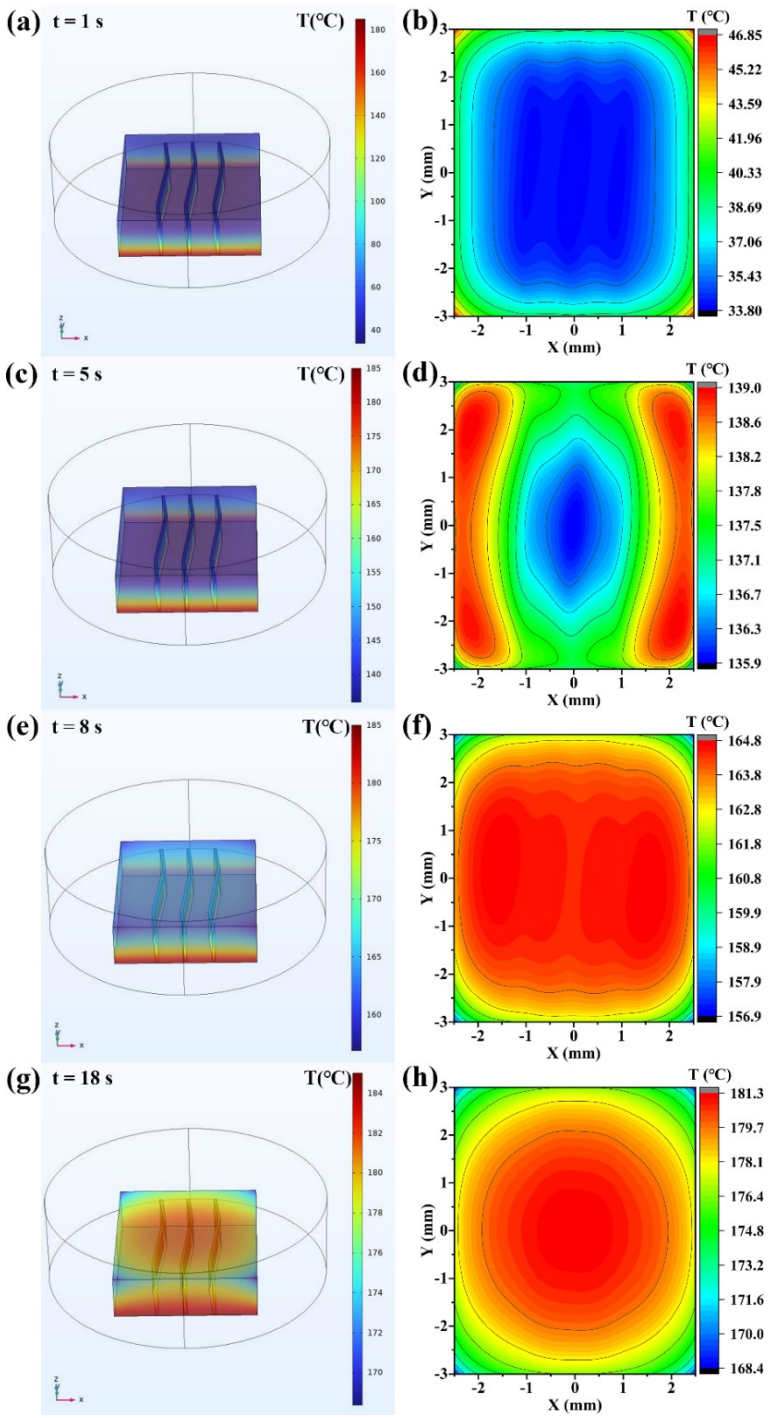

Figure S8 Simulation of the temperature distribution of an HMX crystal containing *fast cracks* with heating time. (a) Temperature distribution of the crystals at 1 s. (b) Temperature distribution of the upper surface of the crystal at 1 s. (c) Temperature distribution of the crystal at 5 s. (d) Temperature distribution of the upper surface of the crystal at 5 s. (e) Temperature distribution of the crystals at 8 s. (f) Temperature distribution of the upper surface of the crystal at 8 s. (g) Temperature distribution of the crystal at 5 s. (g) Temperature distribution of the crystals at 18 s. (h) Temperature distribution of the upper surface of the crystal at 18 s.

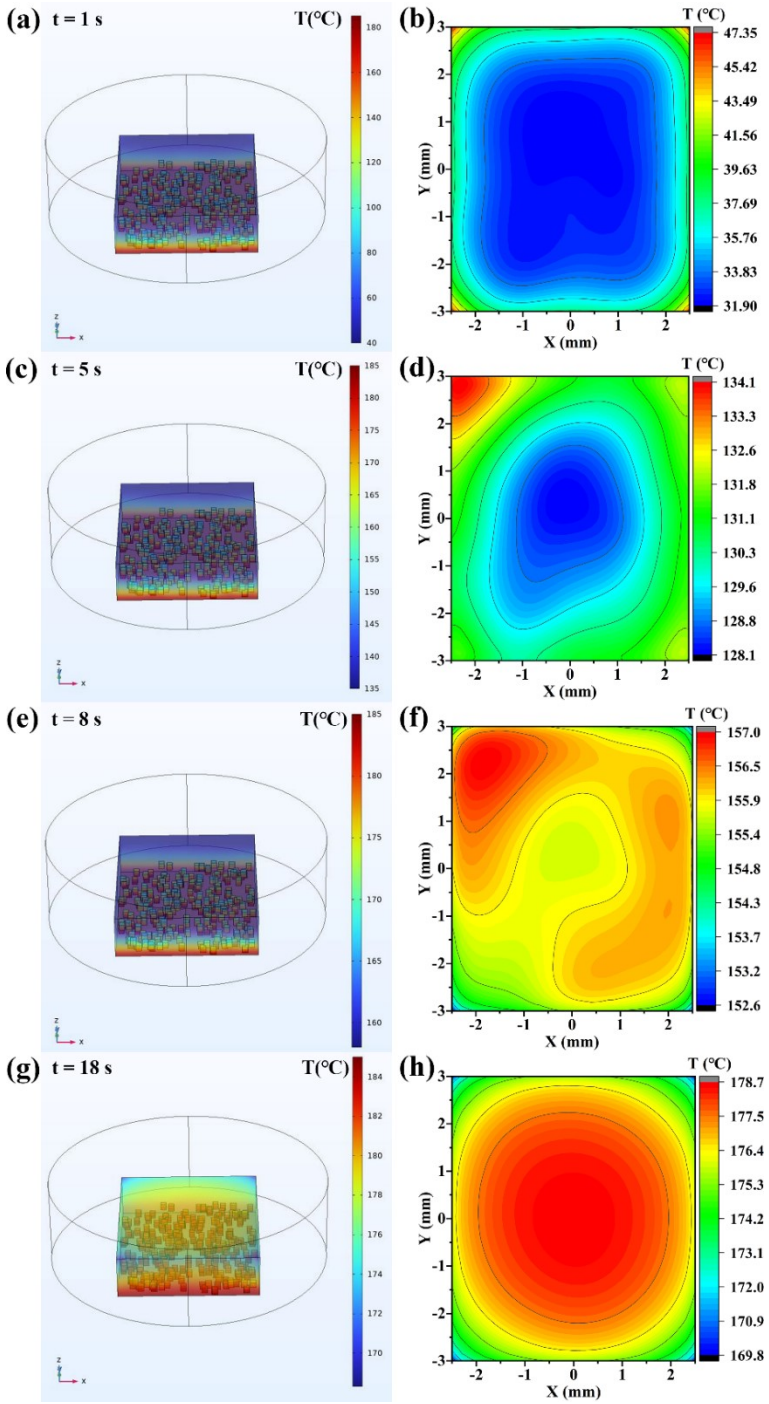

Figure S9 Simulation of the temperature distribution of an HMX crystal containing *small cracks* with heating time. (a) Temperature distribution of the crystals at 1 s. (b) Temperature distribution of the upper surface of the crystal at 1 s. (c) Temperature distribution of the crystal at 5 s. (d) Temperature distribution of the upper surface of the crystal at 5 s. (e) Temperature distribution of the crystals at 8 s. (f) Temperature distribution of the upper surface of the crystal at 8 s. (g) Temperature distribution of the crystal at 5 s. (g) Temperature distribution of the crystals at 18 s. (h) Temperature distribution of the upper surface of the crystal at 18 s.

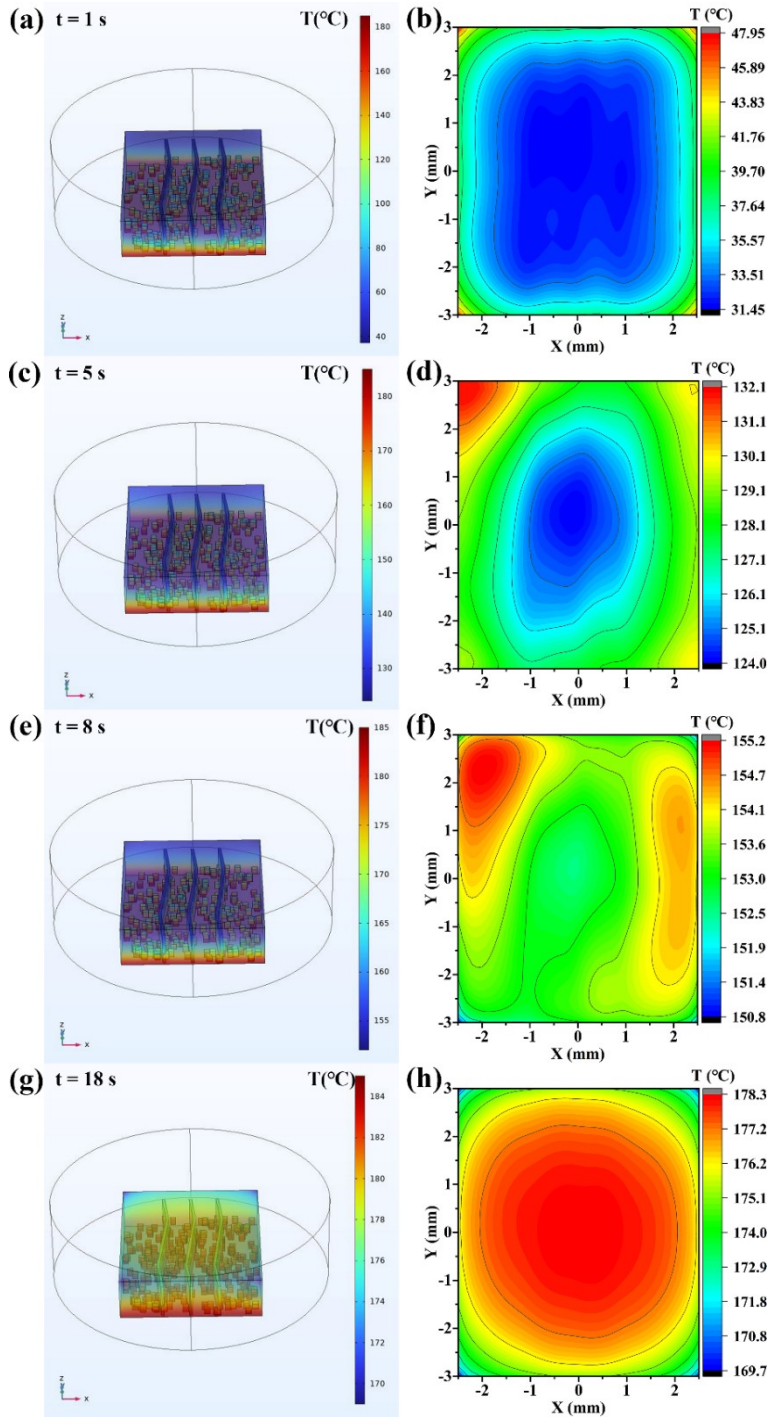

Figure S10 Simulation of the temperature distribution of an HMX crystal containing *fast cracks* and *small cracks* with heating time. (a) Temperature distribution of the crystals at 1 s. (b) Temperature distribution of the upper surface of the crystal at 1 s. (c) Temperature distribution of the crystal at 5 s. (d) Temperature distribution of the upper surface of the crystal at 5 s. (e) Temperature distribution of the crystals at 8 s. (f) Temperature distribution of the upper surface of the crystal at 8 s. (g) Temperature distribution of the crystal at 5 s. (g) Temperature distribution of the crystals at 18 s. (h) Temperature distribution of the upper surface of the crystal at 18 s.

Table S1. Values of initial thermal parameters in the models

Parameters	HMX	Air
ρ (kg/m^3)	1960	1.204
C_p (J/(kg×K))	978	1005.302
λ (W/(m×K))	0.518	0.026

Further detail of the simulation

As shown in Fig. S7 (a), the heating setup in the simulation is divided into the high-temperature furnace cavity, the crystal part and the crack part. The cracks and cavities fully filled with air with initial parameters shown in Table S1. The parameters of HMX were obtained from our measurements and simplified to constants in the model to focus on the effect of cracks, while the relevant parameters for air are the built-in air material parameters in COMSOL following the equation below:

$$\rho = 353.065 \times T^{-1} \ [kg/m^3]$$

$$C_p = 1047.637 - 0.373 \times T + 9.453 \times 10^{-4} \times T^2 - 6.024 \times 10^{-7} \times T^3 + 1.286 \times 10^{-10} \times T^4 \ [J/kg \times K]$$

$$\lambda = -2.276 \times 10^{-3} + 1.155 \times 10^{-4} \times T - 7.903 \times 10^{-8} \times T^2 + 4.117 \times 10^{-11} \times T^3 - 7.439 \times 10^{-15} \times T^4 \ [W/(m \times K)]$$

where T is the value of the temperature in the International System of Units without the unit. The initial temperature of the model is 293.15K (T=293.15), and the bottom of the high temperature chamber is set to a constant temperature of 458.15K (T=458.15) as the only heat source. We set up the convective heat flux coefficient h = 5 W/(m²×K) (normally 5-20 W/(m²×K) in air), as the heat dissipation efficiency of the high temperature cavity boundary except the bottom surface, as shown in Fig. S7 (a). The heat dissipation efficiency q satisfies the following equation:

$$q = h(T_{ext} - T)$$

where T_{ext} is the external temperature constant at 293.15K and T is the temperature at the edge of the high-temperature cavity. The finite element meshing of the model was performed using an extremely fine segmentation with a minimum cell size of about 0.5 μm, as shown in Fig. S7 (b).